Published OnlineFirst December 17, 2010; DOI: 10.1158/0008-5472.CAN-10-2304

Cancer Research

NKX2.2 Suppresses Self-Renewal of Glioma-Initiating Cells

Teruyuki Muraguchi[1], Shingo Tanaka[1,2], Daisuke Yamada[1], Akira Tamase[1,2], Mitsutoshi Nakada[2], Hideo Nakamura[3], Takayuki Hoshii[1], Takako Ooshio[1,4], Yuko Tadokoro[1], Kazuhito Naka[1], Yasushi Ino[5], Tomoki Todo[5], Jun-ichi Kuratsu[3], Hideyuki Saya[6], Jun-ichiro Hamada[2], and Atsushi Hirao[1,4]

Abstract

Glioblastoma (GBM) is the most aggressive and destructive form of brain cancer. Animal models that can unravel the mechanisms underlying its progression are needed to develop rational and effective molecular therapeutic approaches. In this study, we report the development of mouse models for spontaneous gliomas representing distinct progressive stages of disease that are governed by defined genetic alterations. Neural stem/progenitor cell (NPC)-specific constitutive Ras activation *in vivo* plus *p53* deficiency led to development of primarily anaplastic astrocytoma (grade III), whereas combined loss of *p53* plus $p16^{Ink4a}/p19^{Arf}$ led to development of GBM (grade IV) at 100% penetrance within 6 weeks. These glioma models showed enhanced stem cell properties (stemness) accompanied by malignant progression. Notably, we determined that, in our models and in human specimens, downregulation of the homeodomain transcription factor *NKX2.2*, which is essential for oligodendroglial differentiation, was correlated with increased tumor malignancy. *NKX2.2* overexpression by GBM-derived glioma-initiating cells (GIC) induced oligodendroglial differentiation and suppressed self-renewal capacity. By contrast, Nkx2.2 downregulation in mouse NPCs accelerated GBM formation. Importantly, the inhibitory effects of NXK2.2 on GIC self-renewal were conserved in human cells. Thus, our mouse models offer pathobiologically significant advantages to investigate the nature of brain tumors, with improved opportunities to develop novel mechanism-based therapeutic approaches. *Cancer Res; 71(3); 1135–45. ©2010 AACR.*

Introduction

Glioblastoma (GBM) is the most common high-grade malignant glioma in humans and is categorized as a WHO grade IV glioma, a highly aggressive, invasive, and destructive brain tumor (1). There are 2 GBM subtypes, primary and secondary, which are distinguished by clinical characteristics. Primary GBM arises *de novo* in the absence of a preexisting low-grade lesion, whereas secondary GBM develops progressively (over 5–10 years) from lower grade gliomas such as anaplastic astrocytoma (AA, grade III). Alterations in several signaling cascades are known to affect gliomagenesis. These pathways include the receptor tyrosine kinase (RTK)/RAS/PI3K pathway (including EGFR, PDGFR, NF1, and PTEN); the p53 pathway (including TP53, CDKN2A/$p14^{ARF}$, and MDM2); and the RB pathway (including RB1, CDKN2A/$p16^{INK4A}$, CDKN2B and CDKN2C; refs. 1, 2).

Several investigators have developed mouse GBM models by genetically engineering glioma mutations. Reilly and colleagues (3) report a mouse model carrying heterozygous *cis*-germline mutations in the gene encoding a Ras GTPase-activating protein, Nf1, an effector of RTK signaling, in combination with *p53* deficiency. These mice develop malignant gliomas, including GBM and AA, with varying penetrance depending on genetic background (3). Mouse models harboring a heterozygous germline or conditional somatic *p53* mutation combined with conditional somatic *Nf1* heterozygosity develop low- to high-grade astrocytomas (4). Tumor formation is accelerated into high-grade astrocytomas similar to primary GBM by additional loss of *Pten* (5). Concomitant central nervous system (CNS)-specific deletion of *p53* and *Pten* generates a high-grade malignant glioma phenotype ranging from grade III to grade IV, with notable clinical, pathologic, and molecular resemblance to human malignant gliomas (6). Furthermore, Alcantara Llaguno and colleagues (7) have shown that inactivation of Nf1 combined with loss of other tumor suppressors (*p53* and *Pten*) in neural stem/progenitor cells (NPC), but not in non-NPCs, was both necessary and sufficient to induce glioma formation, indicating critical roles

Authors' Affiliations: [1]Division of Molecular Genetics, Cancer and Stem Cell Research Program, Cancer Research Institute and [2]Department of Neurosurgery, Graduate School of Medical Science, Kanazawa University, Kanazawa, Ishikawa, Japan; [3]Department of Neurosurgery, Faculty of Medical and Pharmaceutical Sciences, Kumamoto University Graduate School, Kumamoto, Japan; [4]Core Research for Evolutional Science and Technology (CREST), Japan Science and Technology Agency, Kawaguchi, Saitama, Japan; [5]Department of Neurosurgery and Translational Research Center, Graduate School of Medicine, The University of Tokyo, Tokyo, Japan; and [6]Division of Gene Regulation, Institute for Advanced Medical Research, Keio University School of Medicine, Tokyo, Japan

Note: Supplementary data for this article are available at Cancer Research Online (http://cancerres.aacrjournals.org/).

Corresponding Author: Atsushi Hirao, Division of Molecular Genetics, Cancer and Stem Cell Research Program, Cancer Research Institute, Kanazawa University, Kanazawa, Ishikawa 920-1192, Japan. Phone: 81-76-264-6756; Fax: 81-76-234-4508; E-mail: ahirao@kenroku.kanazawa-u.ac.jp

doi: 10.1158/0008-5472.CAN-10-2304

Published OnlineFirst December 17, 2010; DOI: 10.1158/0008-5472.CAN-10-2304

for Ras activation in NPCs on gliomagenesis *in vivo*. Thus, these mouse models have provided critical information regarding molecular mechanisms underlying gliomagenesis. However, in these models, phenotypic variations in malignant progression are observed even in the presence of the same mutations (5, 7). To better understand mechanisms underlying malignant glioma progression, mouse models that reliably control stages of malignant progression are needed.

Although *RAS* mutations are uncommon in human malignant gliomas, the impact of *NF1* inactivation on human and mouse glioma suggested critical roles of RAS activation in gliomagenesis (8). Proliferation of these tumors requires RAS activation and many of these tumors exhibit elevated RAS signaling, which seems to be central to their pathology (9). Consistent with this notion, several mouse GBM models have been generated by inducing constitutive Ras activation (10–12). In this study, we developed mouse models of gliomagenesis by engineering NPCs to express a constitutively active form of K-Ras via the tamoxifen-induced Cre-loxP system. Interestingly, in combination with loss of the tumor suppressors *p53* and $p16^{Ink4a}/p19^{Arf}$, mutant mice developed glioma at 100% penetrance with short latency (within 10 weeks), a clear alteration in malignant progression status. We also observed a correlation between enhanced stem cell properties (stemness) and malignant progression stages, consistent with human samples. Furthermore, we report that Nkx2.2 is a critical factor controlling self-renewal of glioma-initiating cells (GIC), an activity conserved in human GICs. Our mouse brain tumor models could be used to gain important insights into new therapeutic approaches.

Materials and Methods

Mice

LSL-K-Ras^{G12D} and $p16^{Ink4a+/-}/p19^{Arf+/-}$ mice were obtained from the Mouse Models of Human Cancers Consortium of NCI-Frederick (13, 14). $p53^{+/-}$ and *Nestin-CreER*^{T2} mice were previously described (15, 16). Mice were maintained on a mixed 129SvJ/C57BL/6 background. All animal experiments were approved by the Committee on Animal Experimentation of Kanazawa University and performed in compliance with the University's Guidelines for the Care and Use of Laboratory Animals.

Human brain tumor samples

Tumors from patients with glioma were surgically removed and diagnosed at the Department of Neurosurgery, Kanazawa University and at the Department of Neurosurgery, Kumamoto University. All histologic analyses of NKX2.2 expression levels were performed at low-power magnification, and the entire tissue section was evaluated rather than specific foci or selected high-power fields. NKX2.2 expression levels were scored from negative/weak to positive (>30% of tumor cells), depending on the percentage of $NKX2.2^{+}$ cells in a given tumor. Human GBM patient–derived GICs, termed TGS-01 and TGS-04, were established as described previously (17). All human materials and protocols used in this study were approved by ethics committees of Kanazawa University, Kumamoto University, and the University of Tokyo. Informed consent was obtained from all patients.

Tamoxifen induction

To activate CreER^{T2}*in vivo*, 1 mg tamoxifen (Sigma) in corn oil (Sigma) was administered intraperitoneally to 8-week-old mice once daily for 5 consecutive days. Immunohistochemistry and immunofluorescence analyses were performed on coronal sections of forebrains obtained at 12 weeks of age.

Tissue preparation and histology

Sacrificed mice were perfused with 4% paraformaldehyde (PFA), and brains were dissected and postfixed overnight in 4% PFA at 4°C. Serial sections were prepared at 5 μm for paraffin sections or 10 μm for cryostat sections. Paraffin-embedded mouse brains, mouse gliomas, or human gliomas were deparaffinized and rehydrated prior to immunohistochemical analysis. Tumors were graded according to the WHO grading system for malignant astrocytomas (1).

Antibodies

Immunohistochemistry and immunofluorescence analyses were performed as described (18). Sections were examined using optical, fluorescence, and confocal microscopy (Keyence BZ-9000, Olympus FV1000, and Carl Zeiss Axio Imager A1 microscopes, respectively). Primary antibodies (Abs) recognizing the following proteins were used for immunostaining assays: Nkx2.2 (Developmental Studies Hybridoma Bank; Sigma), Ki-67 (BD), Nestin (BD and Chemicon), Sox2 (Chemicon), CD133 (eBioscience), GFAP (DAKO), Olig2 (Chemicon), βIII-tubulin (Tuj-1, Covance), NG2 (Chemicon), O4 (Chemicon), cleaved caspase-3 (Cell Signaling), HP1γ (Chemicon), γ-H2AX (Upstate), phospho-Akt^{Ser473} (Cell Signaling), CD34 (Chemicon), VEGF (Santa Cruz), PDGFRα (Cell Signaling), myelin basic protein (Mbp; Abcam), and NeuN (Chemicon). Primary Abs were detected using Alexa Fluor-conjugated secondary Abs (Invitrogen), and peroxidase-conjugated secondary Ab (GE Healthcare) plus the DAB Peroxidase Substrate Kit (VECTOR).

Tumor neurospheres

For mouse tumor neurosphere (TNS) formation, mouse glioma cells were isolated from brains of $p53^{-/-}$;NR^{+tamo} or $p53^{-/-}$;$p16^{Ink4a-/-}/p19^{Arf-/-}$;$NR^{+tamo}$ mice. To assay TNS numbers, dissociated cells (2×10^3 cells/200 μL) were seeded into 96-well plates and cultured for 7 days in medium containing 20 ng/mL fibroblast growth factor-2 (FGF-2; Peprotech) and 20 ng/mL epidermal growth factor (EGF; Peprotech) as described (18). TNSs derived from TGS-01 and TGS-04 cells were cultured as described (17). Dissociated cells from sphere preparations were transfected with pLXSB-human *NKX2.2* and cultured as adherent monolayers on poly-L-ornithine–coated coverslips, and then selected in blasticidine-S (8 μg/mL) for 4 days. Transfection was performed using Fugene6 transfection reagent (Roche) according to the manufacturer's instructions. The number of spheres of diameter greater than 50 μm was determined using phase-contrast microscopy.

Published OnlineFirst December 17, 2010; DOI: 10.1158/0008-5472.CAN-10-2304

Retrovirus-mediated Nkx2.2 overexpression

cDNA encoding full-length mouse *Nkx2.2* was cloned into the retroviral vector pLXSB (19). Retroviral packaging cells (Phoenix-E) were transiently transfected as above with pLXSB-*Nkx2.2*. Viral titers were estimated by observing increased drug resistance in infected NIH3T3 cells. TNSs derived from $p53^{-/-}$; $p16^{Ink4a-/-}/p19^{Arf-/-}$;$NR^{+tamo}$ mice were mixed with *Nkx2.2*–expressing viral suspensions and maintained in culture for 7 days, or cultured as adherent monolayers on coverslips with a *Nkx2.2*–expressing virus suspension and then selected in blasticidine-S (8 μg/mL) for 4 days.

Retrovirus-mediated RNA interference

For short hairpin RNA (shRNA)-mediated mRNA knockdown, a retroviral vector (pSM2c) expressing shRNAs under control of the U6 promoter (Open Biosystems) was used. *Nkx2.2* shRNAs were *Nkx2.2* shRNA1 (oligoID: V2HS61850) targeting GGTCAAGATCTGGTTCCAGAA, and *Nkx2.2* shRNA2 (oligoID: V2HS152272) targeting CCAGAACCACCGCTACAAG. Control shRNA was GFP shRNA targeting GCACAAGCTGGAGTACAACTA. NPCs derived from neonatal (P3–5) $p16^{Ink4a-/-}/p19^{Arf-/-}$ mice were cultured as adherent monolayers with a control GFP shRNA or an *Nkx2.2*-shRNA-expressing retrovirus suspension, and then selected with puromycin (2 μg/mL) for 4 days, infected with *EGFRvIII*-expressing retrovirus (pLERNL), and cultured for an additional 7 days. Levels of *Nkx2.2* mRNAs before infection with *EGFRvIII*-expressing retrovirus were determined by quantitative real-time RT-PCR as described in the following section.

Quantitative RT-PCR

RNAs were purified from cultured NPCs using the RNeasy kit (QIAGEN) and reverse-transcribed using the Advantage RT-for-PCR kit (Takara-Clontech). Real-time quantitative PCR was performed using SYBR green Premix EX Taq (Takara) on an Mx3000P real-time PCR system (Aligent Technology). Sense and antisense primers are listed in Supplementary Table S1 online. The following cycle parameters were used: denaturation at 95°C for 10 seconds, and annealing and elongation for 30 seconds at 57°C for *β-actin* and at 60°C for *Nkx2.2*.

Orthotopic transplants

For intracranial injections, TNSs cultured as adherent monolayers were dissociated and resuspended in Hanks Buffered Salt Solution at a concentration of 100,000 viable cells/μL. Female NOD/SCID mice (Charles River) ages 6 to 8 weeks were anesthetized and placed into a stereotactic apparatus equipped with a *z*-axis (Stoelting). A small hole was bored into the skull 0.5 mm anterior and 3.0 mm lateral to bregma using a dental drill. Cell suspensions (2 μL) were injected into the right striatum 3 mm below the surface of the brain using a 10 μL Hamilton syringe with a 26 gauge needle. The scalp was closed using an Autoclip Applier. Animals were monitored daily for neurologic deficits.

Western blotting

Western blotting was performed as described (18). The primary Abs used recognized NKX2.2 (Developmental Studies Hybridoma Bank) or α-tubulin (Sigma).

Statistics

P values were calculated using the unpaired Student's *t* test. Survival curves were plotted using the Kaplan–Meier method, and differences were analyzed using the log-rank test. The significance of the association between NKX2.2 expression and malignancy was determined by the Fisher's exact test (right tail).

Results

Establishment of mouse glioma models that exhibit malignant progression by *in vivo* NPC-specific Ras activation

Because Ras signaling is a major pathway upregulated in gliomagenesis, we asked whether Ras activation in NPCs could induce gliomagenesis *in vivo*. To do so, we established a mouse model in which constitutively activated Ras ($K\text{-}Ras^{G12D}$) could be specifically and temporally induced in NPCs by binding of tamoxifen to a Cre recombinase-modified estrogen receptor ligand-binding domain fusion protein ($Cre\text{-}ER^{T2}$) expressed under control of the *Nestin* promoter/enhancer (13, 15). For these experiments, we designated untreated control *Nestin-CreER*^{T2};*LSL-K-Ras*^{G12D} mice as "NR" mice, tamoxifen-treated NR mice as "NR^{+tamo}" mice, *Nestin-CreER*^{T2} mice treated with tamoxifen as "$control^{+tamo}$" mice, and NR mice treated with vehicle only as "NR^{-tamo}" mice. First, we treated all 4 groups of mice (at 8 weeks of age) with vehicle or tamoxifen and analyzed their brains at 12 weeks of age. Although histologic analysis revealed that the lateral ventricles were slightly enlarged in NR^{+tamo} mice compared with $control^{+tamo}$ and NR^{-tamo} mice, the gross appearance of the brain in all animals was normal (Supplementary Fig. S1). Further analysis indicated that both expression of the proliferation marker Ki-67 antigen and 5-bromodeoxyuridine incorporation were reduced in NR^{+tamo} subventricular zone (SVZ) compared with $control^{+tamo}$ SVZ (Supplementary Fig. S2A–C). Moreover, immunohistochemical analyses showed no differences between NR^{+tamo} and $control^{+tamo}$ SVZ in numbers of $TUNEL^{+}$ apoptotic cells (Supplementary Fig. S3A) or cleaved $caspase\text{-}3^{+}$ cells (Supplementary Fig. S3B). Although it has been shown that oncogenic signaling induces cellular senescence *in vitro* and *in vivo*, we observed no significant differences between $control^{+tamo}$ and NR^{+tamo} SVZ cells in expression of the senescence-associated markers HP1γ or γ-H2AX (Supplementary Fig. S3C), or in SA-β-gal activity (data not shown; ref. 20). Overall we conclude that enlargement of the lateral ventricles observed in NR^{+tamo} mice was largely because of Ras-induced inhibition of NPC proliferation.

NR^{+tamo} mice did not develop tumors, even after long-term observation (Fig. 1A). Therefore, because inactivation of p53 and $p16^{INK4A}/p14^{ARF}$ is commonly seen in human gliomas, we evaluated the impact of loss of these genes on our NR model mice *in vivo*. First, we crossed our NR model mice with *p53* mutant mice. Following administration of tamoxifen, $p53^{-/-}$; NR^{+tamo} mice began dying of brain tumors approximately 6 weeks later, and 100% of the mice were dead by approximately 10 weeks. Histologic analyses of brain tumors revealed that most (9 of 10) were AA, with only 1 of 10 showing classic features of GBM, such as necrosis, microvascular proliferation,

Published OnlineFirst December 17, 2010; DOI: 10.1158/0008-5472.CAN-10-2304

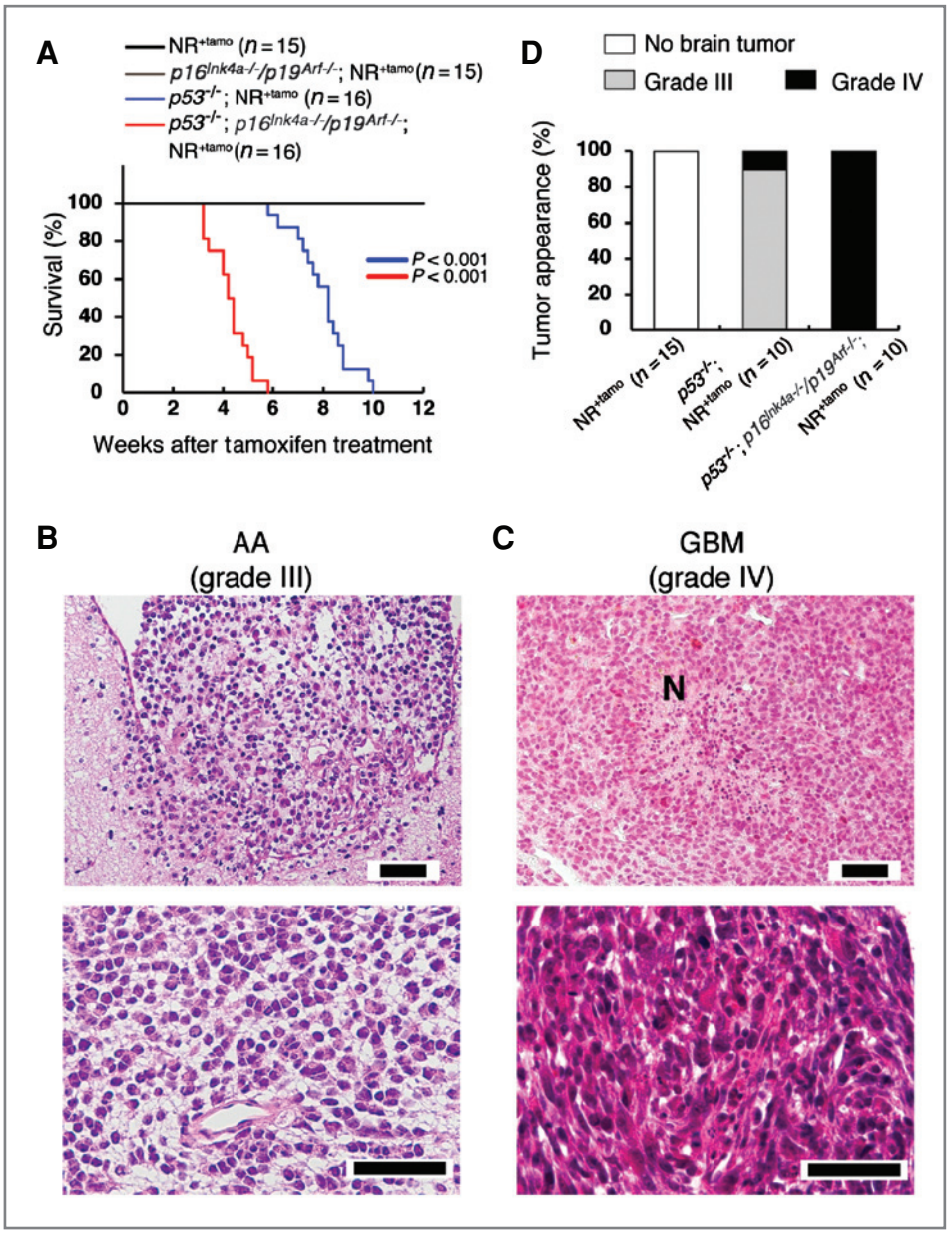

Figure 1. *p53* plus $p16^{Ink4a}/p19^{Arf}$ deficiencies combined with Ras activation drive GBM formation *in vivo*. A, altered survival. Mice of indicated genotypes (8 weeks old) were treated with tamoxifen for 5 days and monitored for tumor development. Kaplan–Meier tumor-free survival curves are shown. B and C, tumor histology. Coronal sections of forebrains of mice in (A) were prepared and stained with H&E. Tumors were graded for severity, as either AA (grade III; B) or GBM (grade IV; C). Scale bars, 50 μm. "N" indicates an area of "palisading" with regional necrosis. Data shown in (B) and (C) are representative of 10 mice/group. D, quantification of (B) and (C). Data shown are the percentage of mice in each group that developed no tumors, or grade III AA, or grade IV GBM.

marked cellular pleomorphism, and highly infiltrative spread to the cerebral cortex (Fig. 1B–D; Supplementary Fig. S4). $p53^{-/-}$;NR^{-tamo} mice did not develop any brain tumors over the period analyzed (data not shown). Next, we crossed our NR model mice with $p16^{Ink4a}/p19^{Arf}$ mutant mice. NR^{+tamo} mice on a $p16^{Ink4a}/p19^{Arf}$ null background also did not develop tumors over the 12-week period analyzed. These findings differ from previous studies showing that cultured NPCs derived from neonatal $p16^{Ink4a-/-}/p19^{Arf-/-}$ mice and infected with retrovirus carrying $K\text{-}Ras^{G12V}$ develop GBMs (10, 21). It was reported that GBM also arises when $p16^{Ink4a-/-}$ or $p19^{Arf-/-}$ mice are engineered to overexpress mutant *K-Ras* gene *in vivo* (10). By contrast to those studies, in our model the mutant *K-Ras* allele is expressed at physiologic levels. Therefore, discrepancies are likely due to differences in the amplitude of oncogenic signaling, the age of the mice used, or the cellular context (transformation *in vitro* or *in vivo*).

To investigate the effect of loss of multiple tumor suppressors in our model, we crossed NR mice with *p53* and $p16^{Ink4a}/p19^{Arf}$ mutant mice. Simultaneous deletion of $p16^{Ink4a}/p19^{Arf}$ plus *p53* significantly shortened the survival time of NR^{+tamo} mice (Fig. 1A). Interestingly, in contrast with $p53^{-/-}$;NR^{+tamo} mice, histologic analyses revealed that 100% of the tumors in $p53^{-/-}$;$p16^{Ink4a-/-}/p19^{Arf-/-}$;$NR^{+tamo}$ mice were GBMs (Fig. 1D). As shown in Figure 2A and C, GBMs derived from $p53^{-/-}$;$p16^{Ink4a-/-}/p19^{Arf-/-}$;$NR^{+tamo}$ mice were phenotypically similar to human GBMs. Those mouse tumors showed markedly increased numbers of $Ki\text{-}67^{+}$ mitotic cells, and expressed the classic human glioma markers glial fibrillary acidic protein (Gfap) and Nestin, and high levels of vascular endothelial

Published OnlineFirst December 17, 2010; DOI: 10.1158/0008-5472.CAN-10-2304

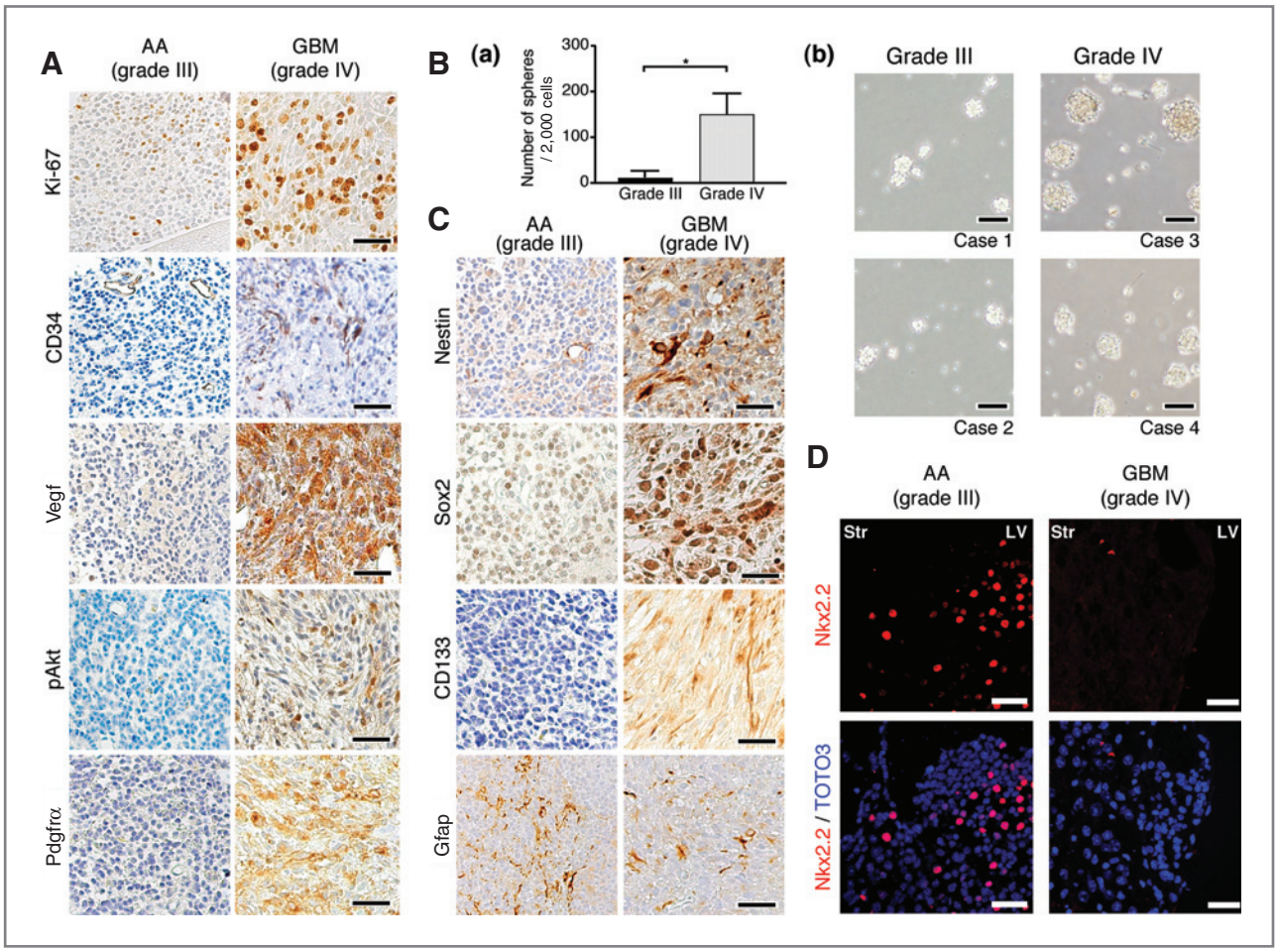

Figure 2. Enhancement of stem cell properties follows malignant glioma progression. A, sections of AAs (grade III) from $p53^{-/-}$;NR^{+tamo} mice and GBMs (grade IV) from $p53^{-/-}$;$p16^{Ink4a-/-}/p19^{Arf-/-}$;$NR^{+tamo}$ mice were immunostained to detect indicated proteins. The resulting staining patterns are highly similar to those seen in human malignant astrocytomas. Scale bars, 100 μm. B, a, increased number of TNSs derived from dissociated mouse GBM cells. b, representative images of the TNSs derived from AAs (grade III, cases 1 and 2) and GBMs (grade IV, cases 3 and 4) are shown. Scale bars, 100 μm. Data shown are the mean number ± SD of TNSs generated per 2,000 cells ($n = 5$/group). *, $P < 0.001$. C, expression of stem cell and glial differentiation markers. Sections of AA (grade III) from $p53^{-/-}$;NR^{+tamo} mice and GBMs (grade IV) from $p53^{-/-}$;$p16^{Ink4a-/-}/p19^{Arf-/-}$;$NR^{+tamo}$ mice were immunostained to detect indicated proteins. The resulting staining patterns are reminiscent of human malignant gliomas. Scale bars, 100 μm. D, expression of oligodendroglial differentiation markers. Forebrain sections from mice in (A) were stained with anti-Nkx2.2 (red) and TOTO3. Str, striatum; LV, lateral ventricle. Scale bars, 25 μm. A, B, and D, results shown are representative of 5 mice/group and 5 experiments.

growth factor (Vegf) and phosphorylated Akt (p-Akt). Coactivation of multiple RTKs, which is often seen in human primary GBMs, was also evident in our murine GBMs, in which we observed markedly upregulated Pdgfrα expression. By contrast, AA seen in $p53^{-/-}$;NR^{+tamo} mice showed only low levels of Ki-67, Nestin, VEGF, p-Akt, and Pdgfrα (Fig. 2A and C). Microvascular formation in mouse GBMs was confirmed by detection of the endothelial marker CD34 (Fig. 2A).

Enhanced stem cell properties (stemness) accompanies malignant progression in mouse glioma models

Previous reports of human GBMs indicate that several stem cell markers, including Nestin, Sox2, and CD133 are upregulated in these malignancies (22–24). Likewise, we found that Nestin, Sox2, and CD133 were upregulated in GBMs from $p53^{-/-}$;$p16^{Ink4a-/-}/p19^{Arf-/-}$;$NR^{+tamo}$ mice, but not in the AA of $p53^{-/-}$;NR^{+tamo} mice (Fig. 2C). Because it has been shown that population of undifferentiated tumor cells known as tumor stem cells, or tumor-initiating cells, can undergo sphere formation *in vitro* (21), we evaluated the capacity of tumor cells in our model to form TNSs in culture by dissociating the entire tumor. A large number of TNSs was generated from cultures of cells derived from dissociated GBM, whereas AA-derived cells produced very few (Fig. 2B), indicating that mouse GBMs, like human GBMs, contain cells exhibiting stem cell properties (stemness).

Given the established inverse relationship between malignant progression and cellular differentiation, we compared expression levels of several differentiation markers in mouse GBM and AA. Consistent with evidence derived from human studies, tumor cells in either $p53^{-/-}$;NR^{+tamo} or $p53^{-/-}$;$p16^{Ink4a-/-}/p19^{Arf-/-}$;$NR^{+tamo}$ mice did not express markers

Published OnlineFirst December 17, 2010; DOI: 10.1158/0008-5472.CAN-10-2304

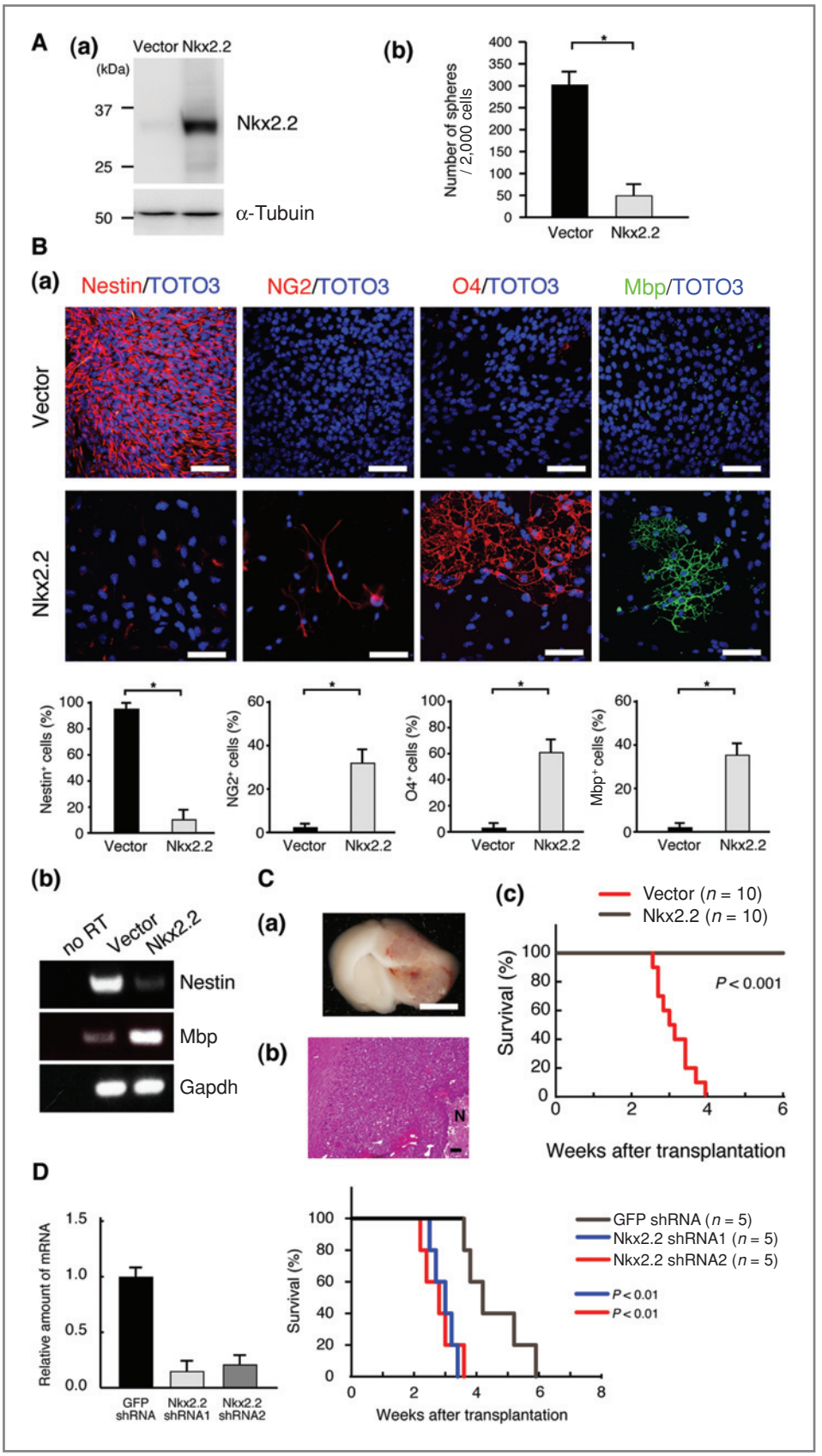

Published OnlineFirst December 17, 2010; DOI: 10.1158/0008-5472.CAN-10-2304

of mature neurons (NeuN; Supplementary Fig. S5). Expression of Mbp or O4, both of which are expressed in mature oligodendrocytes, was not observed in either type of glioma (Supplementary Fig. S5 and data not shown). However, interestingly, Nkx2.2, a homeodomain transcription factor essential for oligodendroglial differentiation, was strongly expressed in AAs but barely detectable in GBMs (Fig. 2D). These data suggest that mechanisms governing oligodendroglial differentiation may play a critical role in regulating malignant progression of glioma.

Nkx2.2 regulates mouse gliomagenesis

Our observation that malignant glioma progression is inversely correlated with loss of Nkx2.2 expression suggested that presence of Nkx2.2 inhibits GBM formation. To test this hypothesis, we assessed the effects of Nkx2.2 upregulation on the fate of GICs within TNSs derived from GBMs. Nkx2.2 reportedly induces oligodendroglial differentiation of normal NPCs (25, 26). We overexpressed Nkx2.2 in dissociated GBM cells derived from $p53^{-/-}$;$p16^{Ink4a-/-}$/$p19^{lArf-/-}$;NR^{+tamo} mice and examined TNS formation. Nkx2.2 overexpression markedly reduced both the numbers of TNSs formed and their expression of Nestin (Fig. 3A and B). Notably, cells within these TNSs showed increased expression of the oligodendrocyte markers, chondroitin sulfate proteoglycan (NG2), O4, and Mbp. These data indicate that Nkx2.2 can induce oligodendroglial differentiation of GICs, decreasing their self-renewal capacity (Fig. 3B). Next we used intracranial injection to introduce vector-transduced murine TNSs into NOD/SCID mice (n = 10), lethal, infiltrating gliomas developed in brains of all mice within 1 month. By contrast, all mice (10 of 10) injected with TNSs overexpressing Nkx2.2 survived for more than 2 months (Fig. 3C). Thus, induction of oligodendroglial differentiation of GICs by Nkx2.2 suppresses GBM formation *in vitro*.

To directly examine the effect of Nkx2.2 loss on gliomagenesis, we assessed the ability of NPCs in which Nkx2.2 was downregulated via shRNA knockdown to promote gliomagenesis in a different genetic murine glioma model, the EGFRvIII-induced GBM model (27). Introduction of *Nkx2.2* shRNA into cultured NPCs from these mice efficiently knocked down *Nkx2.2* expression (Fig. 3D). When recipient mice were inoculated with $p16^{Ink4a-/-}$/$p19^{Arf-/-}$ NPCs expressing EGFRvIII plus *Nkx2.2* shRNA, mouse survival was significantly shorter than that of recipients that received $p16^{Ink4a-/-}$/$p19^{Arf-/-}$ NPCs expressing EGFRvIII plus control shRNA (Fig. 3D). Histologic differences were not observed between gliomas arising from NPCs transduced with control versus *Nkx2.2* shRNAs (data not shown). These data suggest that Nkx2.2 downregulation accelerates formation of lethal GBMs.

NKX2.2 suppresses self-renewal of human GICs by induction of oligodendroglial differentiation *in vitro*

To investigate whether our findings are relevant to human gliomas, we first examined NKX2.2 protein expression in 96 human high-grade gliomas: 33 GBMs, 36 AAs, and 27 anaplastic oligodendrogliomas (AO). As previously reported, immunohistochemical analysis revealed that NKX2.2 was expressed at higher levels in AOs (22 positive cases in 27 AOs, 81%) than the levels in AAs (15 positive cases in 36 AAs, 42%; Fig. 4). Interestingly, most GBMs (28 cases in 33 GBMs) did not express NKX2.2 (Fig. 4). Thus, in both humans and mice, NKX2.2 suppression is positively correlated with increased malignancy in astrocytomas.

To assess the relevance of our findings to human GICs, we examined the effect of NKX2.2 overexpression on TNS formation by GICs. To do so, we used early passage, patient-derived GIC lines, termed TGS-01 and TGS-04, which under serum-free conditions retain phenotypes and genotypes more closely mirroring primary tumor profiles (17). NKX2.2 overexpression markedly reduced both the number of TNS formed from GICs and their expression of Nestin (Fig. 5A–D). In addition, cells within these TNSs showed increased O4 expression. These data indicate that NKX2.2 can decrease self-renewal capacity and induce oligodendroglial differentiation of human GICs *in vitro*, suggesting that mechanisms observed in our mouse models are conserved in human GICs. To examine whether NKX2.2 is directly regulated by transforming growth factor β (TGFβ) or bone morphogenetic protein 4 (BMP) signal, which is involved in maintenance of GICs (17, 28, 29), we examined the effects of the TGFβ inhibitor (SB431542, 1 μmol/L) and BMP4 (100 nmol/L) on NKX2.2 expression in TGS-01 by immunoblotting and immunocytochemistry. NKX2.2 expression was not remarkably affected by these treatments (data not shown) nor was phosphorylation of Smad2/3 and Smad1/5/8 altered by NKX2.2 overexpression. These data suggest that NKX2.2 does not directly interact with TGFβ or BMP signaling in human GICs.

Figure 3. Critical roles of Nkx2.2 in mouse gliomagenesis. A, Nkx2.2 overexpression decreases TNS formation. Primary mouse glioma cells isolated from $p53^{-/-}$;$p16^{Ink4a-/-}$/$p19^{Arf-/-}$;NR^{+tamo} mice were cultured as TNSs, infected with Vector- or Nkx2.2-expressing retrovirus, and cultured for 7 days. a, Western blot analysis of Nkx2.2 protein in representative samples. b, data shown are the mean number ± SD of TNSs generated per 2,000 cells (n = 5/group). *, $P < 0.001$. B, decreased Nestin but increased NG2, O4, and Mbp expression. a, TNSs were cultured on coverslips, infected with Vector- or *Nkx2.2*-expressing retrovirus, selected with blasticidine-S for 4 days, and stained with anti-Nestin (red) plus TOTO3, anti-NG2 (red) plus TOTO3, anti-O4 (red) plus TOTO3, or anti-Mbp (green) plus TOTO3. Data shown represent 5 experiments. Scale bars, 50 μm. Data shown in the bottom are the mean percentage ± SD of $Nestin^+$ or $NG2^+$ or $O4^+$ or Mbp^+ cells among $TOTO3^+$ cells (n = 5/group). *, $P < 0.001$. b, RT-PCR of genes encoding proteins indicated in (a). C, secondary tumors. NOD/SCID mice were injected with retrovirus-infected TNSs cultured as in (B). a, image showing gross appearance of a coronal section from forebrain of a mouse injected with Vector-infected TNS. Data shown represent 10 mice. Scale bar, 3 mm. b, a coronal section of the secondary tumor in (a) stained with H&E. "N" indicates an area of palisading with regional necrosis. Scale bar, 100 μm. c, Kaplan–Meier tumor-free survival curves of NOD/SCID mice injected with TNSs expressing Vector alone or *Nkx2.2*. D, confirmation of shRNA-mediated *Nkx2.2* knockdown (left). SVZ cells from neonatal $p16^{Ink4a-/-}$/$p19^{Arf-/-}$ mice were infected with virus expressing control *GFP* shRNA or the indicated *Nkx2.2* shRNAs. *Nkx2.2* mRNA levels were determined by real-time RT-PCR, normalized to *β-actin* expression, and expressed as arbitrary units relative to control samples (defined as equal to 1). Results shown are the mean ratio ± SD of *Nkx2.2* mRNA relative to *β-actin* (n = 3/group). Right, decreased mouse survival. SVZ cells derived from neonatal $p16^{Ink4a-/-}$/$p19^{Arf-/-}$ mice were cultured, infected with *EGFRvIII*-expressing virus, cultured for 7 more days, and injected into brains of NOD/SCID mice. Kaplan–Meier tumor-free survival curves are shown.

Published OnlineFirst December 17, 2010; DOI: 10.1158/0008-5472.CAN-10-2304

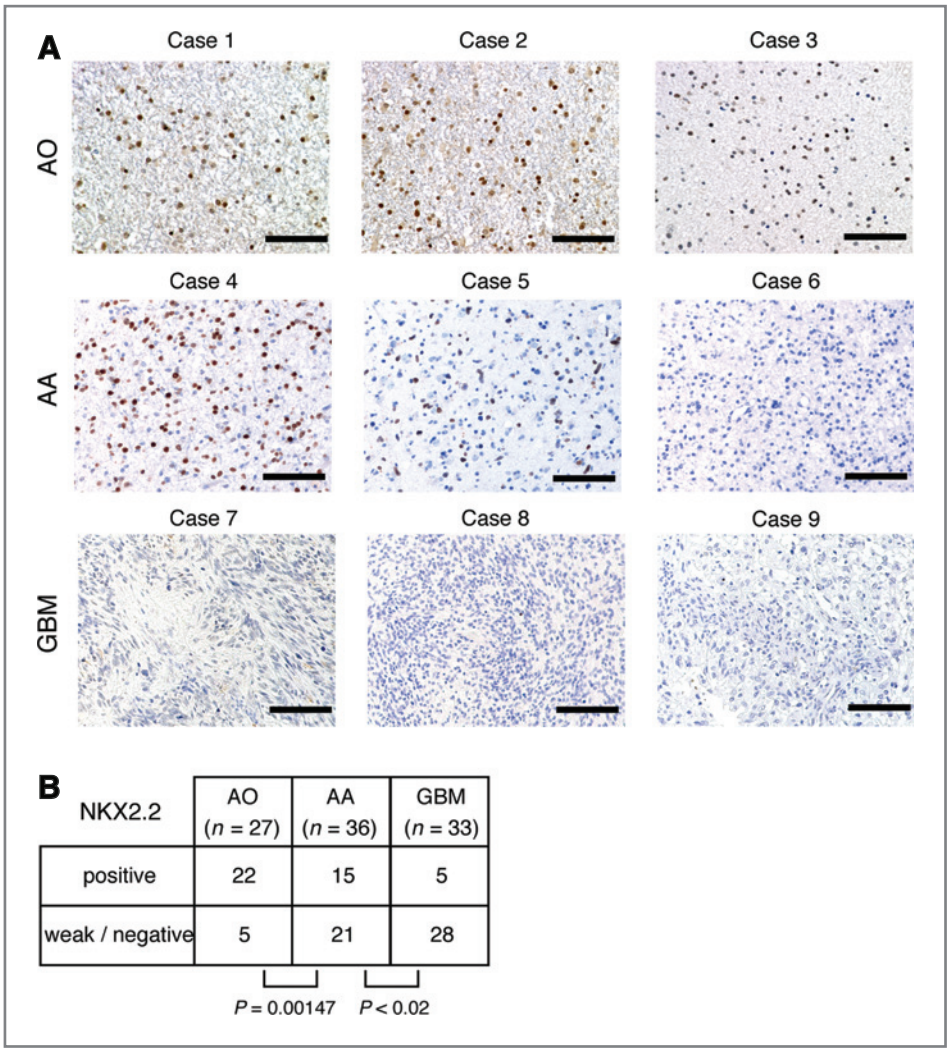

Figure 4. Immunohistochemical examination of NKX2.2 expression in human high-grade gliomas. A, sections of 96 human gliomas were stained with anti-NKX2.2 antibody. Three representative samples of 27 AOs (cases 1–3), 36 AAs (cases 4–6), or 33 GBMs (cases 7–9) are shown. Scale bars, 100 μm. B, correlation between downregulated NKX2.2 expression and malignancy. Gliomas in (A) were scored for intensity of NKX2.2 immunostaining. The significance of the association between the level of NKX2.2 protein expression and malignancy grade was calculated, as determined by Fisher's exact test (right tail).

Discussion

Here, we have established mouse models harboring specific mutations that allow us to control stages of malignant glioma progression (AA versus GBM). These models provide significant advantages in comparing characteristics of gliomas of different malignant progression stages. Mutations seen in human cancers may differ from those seen in mouse models. Nonetheless, mouse models are essential and indispensable to fully understand the nature of gliomas. Our models represent powerful tools useful to identify novel factors that control glioma malignant progression.

A stem cell–like gene expression signature (stemness) has been shown in poorly differentiated tumors, based on histologic criteria. Stemness is associated with an unfavorable prognosis in several human cancers, including gliomas (30). Consistent with these data, we observed enhanced stemness characteristics, including upregulation of stem cell markers or sphere formation, in GBM (grade IV) tumors but not AA (grade III) in our mouse models. Although the mechanism is still unclear, several lines of evidence show that genetic loss of *p53* or $p16^{Ink4a}/p19^{Arf}$ enhances stemness. For example, *p53* or $p16^{Ink4a}/p19^{Arf}$ deficiency increases both the kinetics of induced pluripotent stem (iPS) cell reprogramming and the number of emerging iPS cell colonies (31–35). These results indicate that *p53* and $p16^{Ink4a}/p19^{Arf}$ function as barriers to cell reprogramming and acquisition of stemness. Indeed, *p53*/$p16^{Ink4a}/p19^{Arf}$–deficient multipotent hematopoietic progenitors exhibit properties of hematopoietic stem cells that can carry out long-term reconstitution of blood cells (36). Thus, *p53* and $p16^{Ink4a}/p19^{Arf}$ have a central role in limiting expansion of multipotent progenitors. Because differentiation pathways are commonly repressed in tumor cells, the above results plus our findings suggest a mechanism by which incipient neoplastic cells could gain the ability to self-renew, acquire further oncogenic mutations, and become malignant.

Our study reveals a critical role for Nkx2.2 in suppressing glioma development and GIC self-renewal. A direct effect of Nkx2.2 on oligodendroglial differentiation is supported by previous analyses of mouse spinal cord (25). Coexpression of Olig2 and Nkx2.2 in spinal cord (26) or in the ventricular and

Published OnlineFirst December 17, 2010; DOI: 10.1158/0008-5472.CAN-10-2304

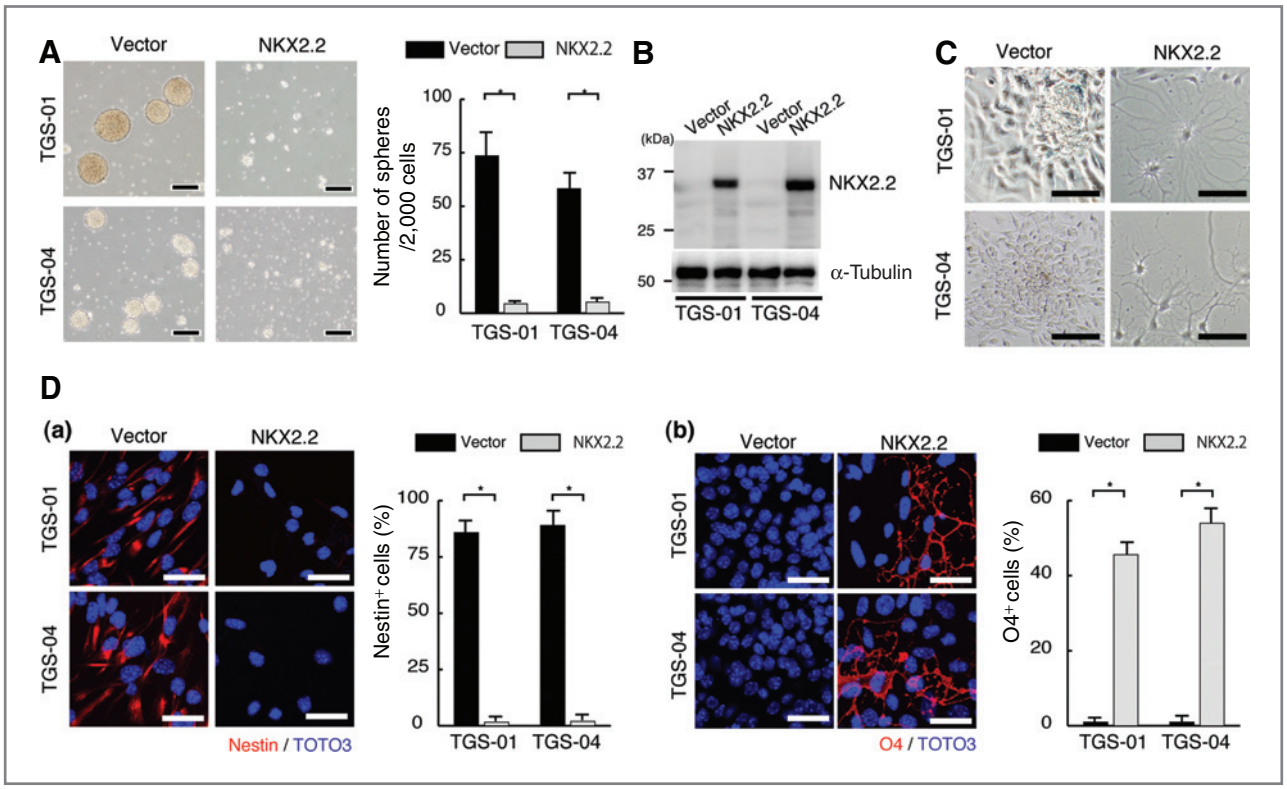

Figure 5. NKX2.2 overexpression inhibits self-renewal of human GICs by induction of oligodendroglial differentiation. A, NKX2.2 overexpression decreases human TNS formation. TGS-01 and TGS-04 cells were cultured as TNSs, transfected with pLXSB (Vector) or pLXSB-*NKX2.2* (NKX2.2), and selected with blasticidine-S for 4 days (left). Scale bars, 100 μm. Right, data shown are the mean number ± SD of TNSs generated per 2,000 cells ($n = 5$/group). *, $P < 0.001$. B, Western blot examination of NKX2.2 protein in representative samples from (A). α-Tubulin: loading control. C and D, decreased Nestin but increased O4 expression. TNSs were cultured on coverslips, transfected with pLXSB (Vector) or pLXSB-*NKX2.2* (NKX2.2), selected with blasticidine-S for 4 days (C, bright-field), and stained with (D, a) anti-Nestin (red) plus TOTO3, or (D, b) anti-O4 (red) plus TOTO3. Data shown represent 5 experiments. Scale bars, 50 μm. Data shown are the mean percentage ± SD of Nestin$^+$ or O4$^+$ cells among TOTO3$^+$ cells ($n = 5$/group). *, $P < 0.001$.

SVZ of the midbrain promotes oligodendrocyte differentiation (37). Olig2 is essential for proliferation and differentiation of oligodendrocyte precursors (38, 39). Olig2-expressing precursors give rise not only to oligodendrocytes but to motor neurons (26, 40), astrocytes, and ependymal cells (41, 42). In contrast to Olig2, Nkx2.2 generally regulates late differentiation and/or maturation, rather than initial specification, of oligodendrocyte precursors (25), although Nkx2.2 does support generation of new oligodendrocytes or remyelination in adults with CNS injury (43, 44). Nkx2.2 cooperates with Olig2 to promote oligodendrocyte maturation to Mbp-positive stages (26, 45). Although several lines of evidence suggest that Olig2 activity represents a mechanistic link between growth of malignant glioma cells and adult NPCs (46, 47), data regarding the role of Nkx2.2 role in gliomagenesis are not available. Our findings suggest that Nkx2.2 functions as a cell fate switch determining whether NPCs receiving oncogenic stimulation develop into benign glial cells or malignant astrocytomas.

Rousseau and colleagues (48) previously reported that NKX2.2 was expressed at higher levels in human AO than in AA and GBMs, suggesting that NKX2.2 is a marker that distinguishes AO from astrocytomas. In addition, it has been reported that NKX2.2 expression is elevated in a proneural subgroup of human GBM (49). In our examination of a larger group of clinically defined samples, we found that NKX2.2 is not only a marker for AO but also an indicator of malignant progression in astrocytomas, suggesting that NKX2.2 expression antagonizes malignant progression of most gliomas. In addition, we showed that impaired oligodendroglial differentiation caused by Nkx2.2 downregulation accelerates GBM formation in a robust murine model of primary gliomagenesis. Our work shows that Nkx2.2 antagonizes glioma initiation and malignant progression induced by activation of oncogenic signaling in NPCs. Finally, we show that forced Nkx2.2 expression in GICs leads to oligodendroglial differentiation and suppression of self-renewal *in vitro*. However, it is unclear whether the inhibitory effects of NKX2.2 on glioma malignancy *in vivo* are mediated by the process of oligodendroglial differentiation, because in both mouse and human samples the mature oligodendrocyte marker, MBP, is not expressed in AA. NKX2.2 may affect malignant progression by an unknown function *in vivo*. Nonetheless, reactivation of NKX2.2 expression in glioma cells suggests a novel therapeutic strategy.

Published OnlineFirst December 17, 2010; DOI: 10.1158/0008-5472.CAN-10-2304

In summary, our novel mouse glioma models allow us to analyze two grades of glioma rapidly and define molecular mechanisms underlying malignant glioma progression. Thus, understanding signaling driving malignant gliomagenesis in our models could contribute to development of novel approaches to diagnose and/or eradicate cancer.

Disclosure of Potential Conflicts of Interest

No potential conflicts of interest were disclosed.

Acknowledgments

We thank Miyako Takegami for expert technical assistance; Drs. Shinichi Aizawa, Itaru Imayoshi, and Ryoichiro Kageyama for providing $p53^{+/-}$ and *Nestin-CreER*^{T2} mice; Dr. Webster K. Cavenee for providing pLERNL plasmids; and Drs. Kenichi Harada, Hiroko Ikeda, and Michiya Sugimori for helpful discussions.

Grant Support

This study was supported by Research Fellowship from the Japan Society for the Promotion of Science for Young Scientists (to T. Muraguchi), grant for cancer research from the Ministry of Education, Culture, Sports, Science and Technology, Japan (to A. Hirao), and grant from the Ministry of Health, Labor and Welfare, Japan, for the Third-Term Comprehensive 10-year Strategy for Cancer Control (to A. Hirao). Part of this work was supported by the Takeda Science Foundation.

The costs of publication of this article were defrayed in part by the payment of page charges. This article must therefore be hereby marked *advertisement* in accordance with 18 U.S.C. Section 1734 solely to indicate this fact.

Received June 28, 2010; revised October 19, 2010; accepted November 14, 2010; published OnlineFirst December 17, 2010.

References

1. Louis DN, Ohgaki H, Wiestler OD, Cavenee WK, editors. WHO classification of tumours of the central nervous system. 4th ed. Lyon, France: World Health Organization; 2007.
2. McLendon R, Friedman A, Bigner D, Van Meir EG, Brat DJ, Mastrogianakis M, et al. Comprehensive genomic characterization defines human glioblastoma genes and core pathways. Nature 2008; 455:1061–8.
3. Reilly KM, Loisel DA, Bronson RT, McLaughlin ME, Jacks T. Nf1;Trp53 mutant mice develop glioblastoma with evidence of strain-specific effects. Nat Genet 2000;26:109–13.
4. Zhu Y, Guignard F, Zhao D, Lui L, Burns DK, Mason RP, et al. Early inactivation of p53 tumor suppressor gene cooperating with NF1 loss induces malignant astrocytoma. Cancer Cell 2005;8:119–30.
5. Kwon CH, Zhao D, Chen J, Alcantara S, Li Y, Burns DK, et al. Pten haploinsufficiency accelerates formation of high-grade astrocytomas. Cancer Res 2008;68: 3286–94.
6. Zheng H, Ying H, Yan H, Kimmelman AC, Hiller DJ, Chen AJ, et al. p53 and Pten control neural and glioma stem/progenitor cell renewal and differentiation. Nature 2008;455: 1129–33.
7. Alcantara Llaguno S, Chen J, Kwon CH, Jackson EL, Li Y, Burns DK, et al. Malignant astrocytomas originate from neural stem/progenitor cells in a somatic tumor suppressor mouse model. Cancer Cell 2009;15:45–56.
8. Huse JT, Holland EC. Targeting brain cancer: advances in the molecular pathology of malignant glioma and medulloblastoma. Nat Rev Cancer 2010;10:319–31.
9. Guha A, Feldkamp MM, Lau N, Boss G, Pawson A. Proliferation of human malignant astrocytomas is dependent on Ras activation. Oncogene 1997;15:2755–65.
10. Uhrbom L, Kastemar M, Johansson FK, Westermark B, Holland EC. Cell type-specific tumor suppression by Ink4a and Arf in Kras-induced mouse gliomagenesis. Cancer Res 2005;65: 2065–9.
11. Marumoto T, Tashiro A, Friedmann-Morvinski D, Scadeng M, Soda Y, Gage FH, et al. Development of a novel mouse glioma model using lentiviral vectors. Nat Med 2009; 15:110–6.
12. Holland EC, Celestino J, Dai C, Schaefer L, Sawaya RE, Fuller GN. Combined activation of Ras and Akt in neural progenitors induces glioblastoma formation in mice. Nat Genet 2000;25:55–7.
13. Tuveson DA, Shaw AT, Willis NA, Silver DP, Jackson EL, Chang S, et al. Endogenous oncogenic K-ras(G12D) stimulates proliferation and widespread neoplastic and developmental defects. Cancer Cell 2004;5:375–87.
14. Serrano M, Lee H, Chin L, Cordon-Cardo C, Beach D, DePinho RA. Role of the INK4a locus in tumor suppression and cell mortality. Cell 1996;85:27–37.
15. Imayoshi I, Ohtsuka T, Metzger D, Chambon P, Kageyama R. Temporal regulation of Cre recombinase activity in neural stem cells. Genesis 2006;44:233–8.
16. Tsukada T, Tomooka Y, Takai S, Ueda Y, Nishikawa S, Yagi T, et al. Enhanced proliferative potential in culture of cells from p53-deficient mice. Oncogene 1993;8:3313–22.
17. Ikushima H, Todo T, Ino Y, Takahashi M, Miyazawa K, Miyazono K. Autocrine TGF-beta signaling maintains tumorigenicity of glioma-initiating cells through Sry-related HMG-box factors. Cell Stem Cell 2009;5:504–14.
18. Muraguchi T, Takegami Y, Ohtsuka T, Kitajima S, Chandana EP, Omura A, et al. RECK modulates Notch signaling during cortical neurogenesis by regulating ADAM10 activity. Nat Neurosci 2007; 10:838–45.
19. Miki T, Takegami Y, Okawa K, Muraguchi T, Noda M, Takahashi C. The reversion-inducing cysteine-rich protein with Kazal motifs (RECK) interacts with membrane type 1 matrix metalloproteinase and CD13/aminopeptidase N and modulates their endocytic pathways. J Biol Chem 2007;282:12341–52.
20. Collado M, Gil J, Efeyan A, Guerra C, Schuhmacher AJ, Barradas M, et al. Tumour biology: senescence in premalignant tumours. Nature 2005;436:642.
21. Tamase A, Muraguchi T, Naka K, Tanaka S, Kinoshita M, Hoshii T, et al. Identification of tumor-initiating cells in a highly aggressive brain tumor using promoter activity of nucleostemin. Proc Natl Acad Sci U S A 2009;106:17163–8.
22. Pfenninger CV, Roschupkina T, Hertwig F, Kottwitz D, Englund E, Bengzon J, et al. CD133 is not present on neurogenic astrocytes in the adult subventricular zone, but on embryonic neural stem cells, ependymal cells, and glioblastoma cells. Cancer Res 2007;67:5727–36.
23. Gangemi RM, Griffero F, Marubbi D, Perera M, Capra MC, Malatesta P, et al. SOX2 silencing in glioblastoma tumor-initiating cells causes stop of proliferation and loss of tumorigenicity. Stem Cells 2009;27:40–8.
24. Strojnik T, Rosland GV, Sakariassen PO, Kavalar R, Lah T. Neural stem cell markers, nestin and musashi proteins, in the progression of human glioma: correlation of nestin with prognosis of patient survival. Surg Neurol 2007;68:133–43;discussion 43–4.
25. Qi Y, Cai J, Wu Y, Wu R, Lee J, Fu H, et al. Control of oligodendrocyte differentiation by the Nkx2.2 homeodomain transcription factor. Development 2001; 128:2723–33.
26. Zhou Q, Choi G, Anderson DJ. The bHLH transcription factor Olig2 promotes oligodendrocyte differentiation in collaboration with Nkx2.2. Neuron 2001;31:791–807.
27. Bachoo RM, Maher EA, Ligon KL, Sharpless NE, Chan SS, You MJ, et al. Epidermal growth factor receptor and Ink4a/Arf: convergent mechanisms governing terminal differentiation and transformation along the neural stem cell to astrocyte axis. Cancer Cell 2002; 1:269–77.
28. Piccirillo SG, Reynolds BA, Zanetti N, Lamorte G, Binda E, Broggi G, et al. Bone morphogenetic proteins inhibit the tumorigenic potential of human brain tumour-initiating cells. Nature 2006;444:761–5.

29. Penuelas S, Anido J, Prieto-Sanchez RM, Folch G, Barba I, Cuartas I, et al. TGF-beta increases glioma-initiating cell self-renewal through the induction of LIF in human glioblastoma. Cancer Cell 2009;15:315–27.
30. Ben-Porath I, Thomson MW, Carey VJ, Ge R, Bell GW, Regev A, et al. An embryonic stem cell-like gene expression signature in poorly differentiated aggressive human tumors. Nat Genet 2008;40:499–507.
31. Li H, Collado M, Villasante A, Strati K, Ortega S, Canamero M, et al. The Ink4/Arf locus is a barrier for iPS cell reprogramming. Nature 2009;460:1136–9.
32. Marion RM, Strati K, Li H, Murga M, Blanco R, Ortega S, et al. A p53-mediated DNA damage response limits reprogramming to ensure iPS cell genomic integrity. Nature 2009;460:1149–53.
33. Hong H, Takahashi K, Ichisaka T, Aoi T, Kanagawa O, Nakagawa M, et al. Suppression of induced pluripotent stem cell generation by the p53-p21 pathway. Nature 2009;460:1132–5.
34. Utikal J, Polo JM, Stadtfeld M, Maherali N, Kulalert W, Walsh RM, et al. Immortalization eliminates a roadblock during cellular reprogramming into iPS cells. Nature 2009;460:1145–8.
35. Kawamura T, Suzuki J, Wang YV, Menendez S, Morera LB, Raya A, et al. Linking the p53 tumour suppressor pathway to somatic cell reprogramming. Nature 2009; 460:1140–4.
36. Akala OO, Park IK, Qian D, Pihalja M, Becker MW, Clarke MF. Long-term haematopoietic reconstitution by Trp53-/-p16Ink4a-/-p19Arf-/- multipotent progenitors. Nature 2008;453:228–32.
37. Fu H, Cai J, Rutledge M, Hu X, Qiu M. Oligodendrocytes can be generated from the local ventricular and subventricular zones of embryonic chicken midbrain. Brain Res Dev Brain Res 2003; 143:161–5.
38. Zhou Q, Wang S, Anderson DJ. Identification of a novel family of oligodendrocyte lineage-specific basic helix-loop-helix transcription factors. Neuron 2000;25:331–43.
39. Lu QR, Yuk D, Alberta JA, Zhu Z, Pawlitzky I, Chan J, et al. Sonic hedgehog–regulated oligodendrocyte lineage genes encoding bHLH proteins in the mammalian central nervous system. Neuron 2000;25:317–29.
40. Lu QR, Sun T, Zhu Z, Ma N, Garcia M, Stiles CD, et al. Common developmental requirement for Olig function indicates a motor neuron/oligodendrocyte connection. Cell 2002;109:75–86.
41. Masahira N, Takebayashi H, Ono K, Watanabe K, Ding L, Furusho M, et al. Olig2-positive progenitors in the embryonic spinal cord give rise not only to motoneurons and oligodendrocytes, but also to a subset of astrocytes and ependymal cells. Dev Biol 2006;293:358–69.
42. Marshall CA, Novitch BG, Goldman JE. Olig2 directs astrocyte and oligodendrocyte formation in postnatal subventricular zone cells. J Neurosci 2005;25:7289–98.
43. Watanabe M, Hadzic T, Nishiyama A. Transient upregulation of Nkx2.2 expression in oligodendrocyte lineage cells during remyelination. Glia 2004;46:311–22.
44. Fancy SP, Zhao C, Franklin RJ. Increased expression of Nkx2.2 and Olig2 identifies reactive oligodendrocyte progenitor cells responding to demyelination in the adult CNS. Mol Cell Neurosci 2004;27: 247–54.
45. Sun T, Dong H, Wu L, Kane M, Rowitch DH, Stiles CD. Cross-repressive interaction of the Olig2 and Nkx2.2 transcription factors in developing neural tube associated with formation of a specific physical complex. J Neurosci 2003;23:9547–56.
46. Ligon KL, Huillard E, Mehta S, Kesari S, Liu H, Alberta JA, et al. Olig2-regulated lineage-restricted pathway controls replication competence in neural stem cells and malignant glioma. Neuron 2007;53:503–17.
47. Tabu K, Ohnishi A, Sunden Y, Suzuki T, Tsuda M, Tanaka S, et al. A novel function of OLIG2 to suppress human glial tumor cell growth via p27Kip1 transactivation. J Cell Sci 2006;119:1433–41.
48. Rousseau A, Nutt CL, Betensky RA, Iafrate AJ, Han M, Ligon KL, et al. Expression of oligodendroglial and astrocytic lineage markers in diffuse gliomas: use of YKL-40, ApoE, ASCL1, and NKX2–2. J Neuropathol Exp Neurol 2006;65:1149–56.
49. Verhaak RG, Hoadley KA, Purdom E, Wang V, Qi Y, Wilkerson MD, et al. Integrated genomic analysis identifies clinically relevant subtypes of glioblastoma characterized by abnormalities in PDGFRA, IDH1, EGFR, and NF1. Cancer Cell; 17:98–110.

Cancer Research
The Journal of Cancer Research (1916–1930) | The American Journal of Cancer (1931–1940)

AACR American Association for Cancer Research

NKX2.2 Suppresses Self-Renewal of Glioma-Initiating Cells

Teruyuki Muraguchi, Shingo Tanaka, Daisuke Yamada, et al.

Cancer Res 2011;71:1135-1145. Published OnlineFirst December 17, 2010.